

80-FM-39

JSC-16758

AUG 7 1980

# Orbit IMU <sup>ALIGNMENT</sup> ~~Alignment~~: Error Analysis

(NASA-TM-91030) ORBIT IMU ALIGNMENT: ERROR N80-28415  
ANALYSIS (NASA) 42 p HC A03/MF A01 CSCL 20A

Unclas  
G3/17 26922

Mission Planning and Analysis Division

August 1980

# NASA

National Aeronautics and  
Space Administration

Lyndon B. Johnson Space Center  
Houston, Texas



SHUTTLE PROGRAM

*Alignment*  
ORBIT IMU ~~ALIGNMENT~~: ERROR ANALYSIS

By R. W. Corson, McDonnell Douglas Technical Services Co.

JSC Task Monitor: T. J. Blucker, Mathematical Physics Branch

Approved: *Emil Schiesser*  
Emil Schiesser, Chief  
Mathematical Physics Branch

Approved: *Ronald L. Berry*  
Ronald L. Berry, Chief  
Mission Planning and Analysis Division

Mission Planning and Analysis Division  
National Aeronautics and Space Administration  
Lyndon B. Johnson Space Center  
Houston, Texas  
August 1980

CONTENTS

Section	Page
1.0 <u>SUMMARY</u> . . . . .	1
2.0 <u>INTRODUCTION</u> . . . . .	2
3.0 <u>DISCUSSION</u> . . . . .	4
4.0 <u>RESULTS</u> . . . . .	6
4.1     THE RMS IMU ALIGNMENT ERROR . . . . .	6
4.2     THE SINGLE AXIS IMU ALIGNMENT ERROR . . . . .	8
4.3     THE MAXIMUM EXPECTED IMU ALIGNMENT ERROR . . . . .	12
4.4     THE STS-1 CASE . . . . .	13
4.5     SPECIAL CASES . . . . .	13
5.0 <u>CONCLUSIONS AND RECOMMENDATIONS</u> . . . . .	16
5.1     CREW PROCEDURES . . . . .	16
6.0 <u>REFERENCES</u> . . . . .	18
APPENDIX A - STAR TRACKER, IMU, AND NAV BASE ERROR MODEL PARAMETERS . .	19
APPENDIX B - MONTE CARLO SIMULATION DERIVED IMU ALIGNMENT ERROR STATISTICS . . . . .	21
APPENDIX C - TOTAL AND SINGLE-AXIS IMU ALIGNMENT ERROR PROBABILITY DENSITY FUNCTIONS FOR STS-1 TYPE ALIGNMENTS . . . . .	28
APPENDIX D - DERIVATION OF THE RMS IMU ALIGNMENT ERROR INDICATOR . . .	33
D.0     THE RMS IMU ALIGNMENT ERROR . . . . .	34
D.1     DERIVATION OF ALIGNMENT ERROR INDICATOR . . . . .	34
D.2     THE STS-1 CASE . . . . .	36

TABLES

Table		Page
4.0-1	IMU ALIGNMENT ACCURACY INDICATORS . . . . .	6
4.1-1	RMS TOTAL IMU ALIGNMENT ERROR . . . . .	7
4.5-1	RMS ALIGNMENT ERROR - SPECIAL CASES . . . . .	15
B-1	KEY TO SIMULATION PROGRAM OUTPUTS . . . . .	22
B-2	IMU ALIGNMENT ERROR STATISTICS FOR 90° STAR PAIR ANGULAR SEPARATIONS . . . . .	23
B-3	IMU ALIGNMENT ERROR STATISTICS FOR 75° STAR PAIR ANGULAR SEPARATIONS . . . . .	24
B-4	IMU ALIGNMENT ERROR STATISTICS FOR 60° STAR PAIR ANGULAR SEPARATIONS . . . . .	25
B-5	IMU ALIGNMENT ERROR STATISTICS FOR 45° STAR PAIR ANGULAR SEPARATIONS . . . . .	26
B-6	IMU ALIGNMENT ERROR STATISTICS FOR 30° STAR PAIR ANGULAR SEPARATIONS . . . . .	27

FIGURES

Figure		Page
2.0-1	IMU ALIGNMENT COORDINATE SYSTEMS AND TRANSFORMATIONS . . . .	3
4.1-1	RMS IMU ALIGNMENT ERROR . . . . .	9
4.2-1	STANDARD DEVIATION OF THE SINGLE AXIS IMU ALIGNMENT ERROR . .	11
4.3-1	ESTIMATED MAXIMUM TOTAL IMU ALIGNMENT ERROR . . . . .	14
C-1	TOTAL IMU ALIGNMENT ERROR PROBABILITY DENSITY FUNCITON . . .	29
C-2	X-AXIS IMU ALIGNMENT ERROR PROBABILITY DENSITY FUNCTION . . .	30
C-3	Y-AXIS IMU ALIGNMENT ERROR PROBABILITY DENSITY FUNCTION . . .	31
C-4	Z-AXIS IMU ALIGNMENT ERROR PROBABILITY DENSITY FUNCTION . . .	32

## 1.0 SUMMARY

A comprehensive accuracy analysis of orbit IMU alignments using the Shuttle star trackers has been completed and the results are presented herein. Monte Carlo techniques were used in a computer simulation of the IMU alignment hardware and software systems to: (1) determine the expected STS-1 (manual mode) IMU alignment accuracy, (2) investigate the accuracy of alignments in later Shuttle flights when the automatic mode of star acquisition may be used, and (3) verify that an analytical model previously used for estimating the alignment error is a valid model.

In summary, the analysis results do not differ significantly from expectations. The standard deviation in the IMU alignment error for STS-1 alignments was determined to be 68 arc seconds per axis. This corresponds to a 99.7% probability that the magnitude of the total alignment error is less than 258 arc seconds.

## 2.0 INTRODUCTION

IMU alignments are performed in order to reposition each IMU inertial platform to a desired orientation with respect to the Mean of 1950 coordinate system. The platforms must be realigned periodically because they do not remain perfectly inertial but drift away from their desired orientations. Figure 2.0-1 illustrates the various coordinate systems associated with the IMU alignment. Each circle represents a coordinate system and the connecting lines represent coordinate transformations. In order to reposition a platform, its present orientation must first be determined. This can be accomplished by measuring the positions of two stars relative to the platform. The star measurements are nominally acquired by using the star trackers (ST). The Mean-of-1950 to measured IMU platform transformation matrix,  $M$ , is determined from these two star measurements (Reference 1). The measured transformation matrix,  $M$ , is different from the actual transformation matrix,  $A$ , due to the star tracker and IMU measurement errors. Next, a platform repositioning matrix,  $T$ , is computed from

$$T = RM^T \quad (1)$$

where the matrix  $R$  defines the transformation from the Mean-of-1950 coordinate system to the desired IMU platform orientation. Finally, IMU torquing commands are extracted from this matrix and applied to the IMU. Note that the torquing angles are applied to the actual IMU; therefore, the final orientation of the IMU will not coincide with the desired orientation. The angular displacement between the repositioned IMU platform and the desired orientation is referred to as the IMU alignment error. Assuming there are no errors associated with the torquing of the IMU, the alignment error transformation matrix, denoted by  $TET^T$  in Figure 2.0-1, is similar to the transformation matrix  $E$ . In other words, both transformations represent the same eigenaxis rotation in inertial space. The alignment error matrix  $E$  can be computed from

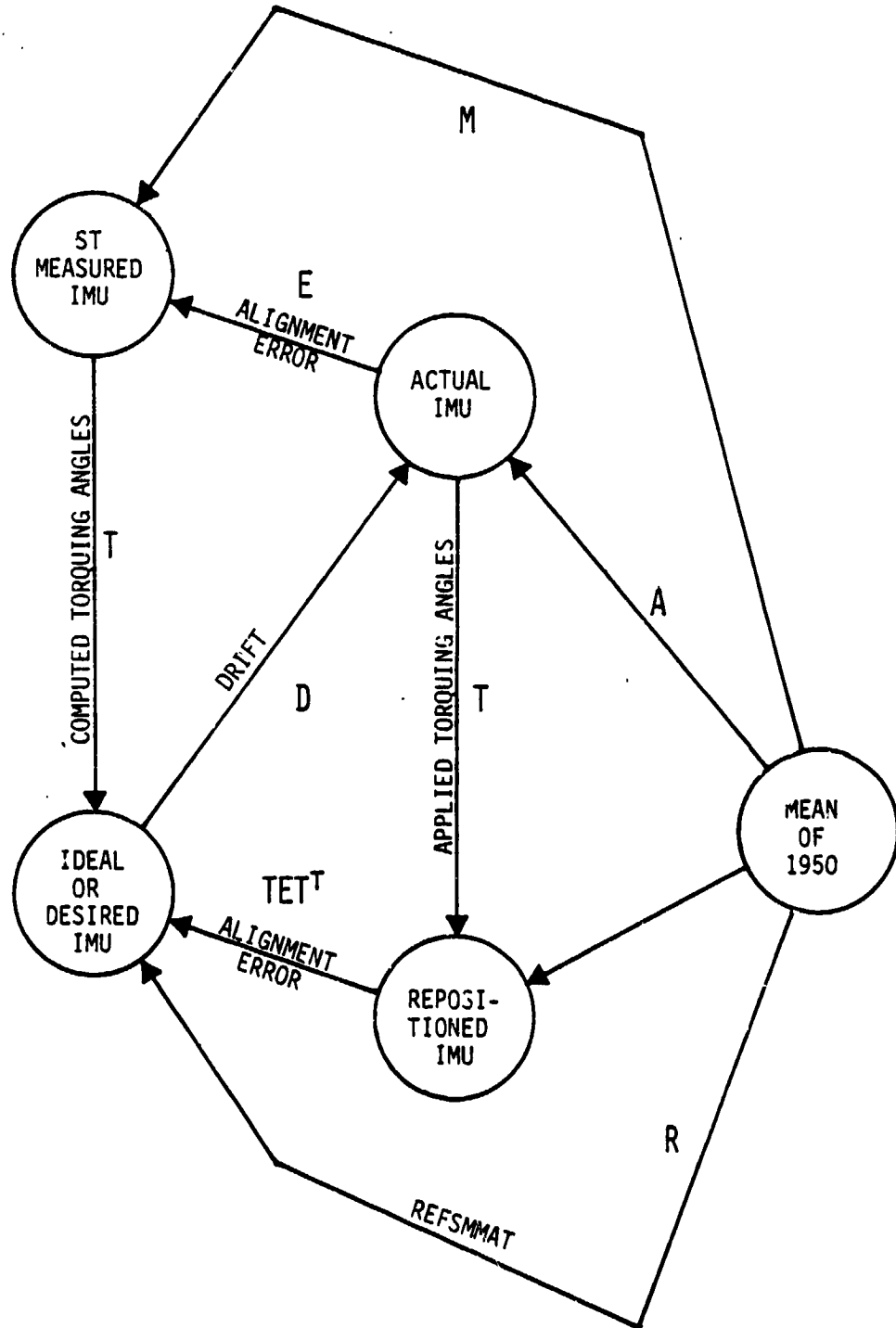
$$E = MA^T \quad (2)$$

assuming that the actual platform orientation matrix  $A$  is known.

In this analysis, the IMUCAL simulation program was used to determine the properties of the IMU alignment error matrix  $E$  using Monte Carlo techniques.

ORIGINAL PAGE IS  
OF POOR QUALITY

FIGURE 2.0-1 IMU ALIGNMENT COORDINATE SYSTEMS AND TRANSFORMATIONS





### 3.0 DISCUSSION

The IMUCAL simulation program has been modified to compile statistical data on IMU alignment accuracy for multiple sample cases. For each alignment sample (one Monte Carlo cycle), an alignment error matrix E is computed from equation 2. The Mean-of-1950 to measured platform transformation matrix M is computed as an intermediate step in the onboard alignment process while the actual platform orientation matrix A is available from the environment. Once the error matrix E is determined, an alignment error vector  $\phi$  is then computed as follows:

$$\phi = 2 \frac{Q}{|Q|} \sin^{-1} |Q| \quad (3)$$

where

$$Q = \frac{1}{2\sqrt{1 + E_{11} + E_{22} + E_{33}}} \begin{bmatrix} E_{23} - E_{32} \\ E_{31} - E_{13} \\ E_{12} - E_{21} \end{bmatrix} \quad (4)$$

denotes the vector part of a quaternion equivalent to the alignment error matrix E. The vector  $\phi$  defines the magnitude and direction of the angular displacement of the measured IMU platform with respect to the actual platform orientation. Note that  $\phi$  is expressed in the actual platform coordinate system. For each case, the simulation program computes the mean and the standard deviation of each of the alignment error vector components  $\phi_x$ ,  $\phi_y$ ,  $\phi_z$  as well as the alignment error vector magnitude  $|\phi|$ . These statistics were computed using the following equations ( $k$  = number of samples).

MEAN (per axis,  $j = x, y, z$ )

$$\mu_j = \frac{1}{k} \sum_{i=1}^k (\phi_j)_i \quad (5)$$

STANDARD DEVIATION (per axis,  $j = x, y, z$ )

$$\sigma_j = \sqrt{\frac{1}{k-1} \left[ \sum_{i=1}^k (\phi_j^2)_i - \frac{1}{k} \left( \sum_{i=1}^k (\phi_j)_i \right)^2 \right]} \quad (6)$$

MEAN (total)

$$\mu = \frac{1}{k} \sum_{i=1}^k (|\phi|)_i \quad (7)$$

STANDARD DEVIATION (total)

$$\sigma = \sqrt{\frac{1}{k-1} \left[ \sum_{i=1}^k (|\phi|^2)_i - \frac{1}{k} \left( \sum_{i=1}^k (|\phi|)_i \right)^2 \right]} \quad (8)$$

A total of eighteen different IMU alignment cases were simulated. In each case, 100 samples of the IMU alignment error  $\Phi$  were generated for each IMU. These cases, which are presented in Table 4.1-1, simulated various combinations of star pair spatial separations ( $\delta$ ) and temporal separations ( $t$ ). The STS-1 trajectory (cycle 2) was simulated in every case and the simultaneous right angle pair case (case 1) conformed to the first STS-1 orbit alignment in detail. The selected alignment stars were Achernar and Alpheratz which were sighted simultaneously at 2:45 GET by the -Z and the -Y star trackers, respectively. The remaining cases simulated alignments for later flights when the automatic mode of star acquisition may be used. In the automatic mode, stars of opportunity are acquired under software direction and a wide range of spatial and temporal separations are possible. Software alignment star selection limits the separation ranges to

$$35^{\circ} \leq \delta \leq 145^{\circ}$$

$$0 \leq t \leq 90 \text{ minutes}$$

The temporal separation limit (sighting age limit) is applied only when data for four stars are available.

For this analysis, angular pair separations between 30 degrees and 90 degrees and temporal separations less than 90 minutes were investigated. Angular separations greater than 90 degrees were not simulated because the alignment error function is symmetric with respect to right angle separations (see Section 4.0).

For each sample, the IMU, ST, and Navigation Base bias errors were initialized at random, based on current estimates of the hardware system performance (Appendix A). Initialization also included the positioning of the three IMU's in a random inertial orientation with a fixed relative skew. Each IMU had 2 hours and 45 minutes of accumulated bias drift error at the time of the first star sighting. In those cases where a finite temporal separation was simulated, the first star was sighted by the -Z star tracker at 2:45 GET. After the desired amount of time had elapsed (30-90 minutes), an attitude maneuver was executed to place the second star in the -Y star tracker field of view (FOV). In each case, the alignment was performed immediately after the sighting of the second star. The second star measurement, therefore, was not corrupted by IMU drift error.

#### 4.0 RESULTS

Detailed simulation results for each analysis case are given in Tables B-1 through B-6 in Appendix B. Since several alignment error indicators are used an explanation of each is given below and summarized in Table 4.0-1. The mean and standard deviation are defined by equations 5 - 8.

TABLE 4.0-1 IMU Alignment Accuracy Indicators

	PER AXIS INDICATORS	3 AXIS OR TOTAL ERROR INDICATORS
MEAN	$\mu_x, \mu_y, \mu_z$	$\mu$
STANDARD DEVIATION	$\sigma_x, \sigma_y, \sigma_z$	$\sigma$
RMS	$\omega_0$	$\omega$

#### 4.1 THE RMS IMU ALIGNMENT ERROR

The root mean square (RMS) indicator

$$\omega = \sqrt{E(|\phi|^2)} = \sqrt{\mu^2 + \sigma^2} \quad (9)$$

can be expressed in terms of the spatial and temporal star pair separations, the variance of the single axis star sighting measurement error  $\sigma_0^2$ , and the variance of the single axis IMU platform drift rate  $\sigma_d^2$  as follows (see Appendix D for derivation).

$$\omega = \sqrt{\sigma_0^2 (1 + 2 \csc^2 \delta) + \sigma_d^2 t^2 \csc^2 \delta} \quad (10)$$

As can be seen from this equation, an optimum value of the alignment error occurs for a spatial separation of 90 degrees and a temporal separation of zero. The RMS indicator is suitable for estimating the IMU alignment accuracy since in a single number, it includes a measure of both the mean error and the variance of the error. It is also valid for use in the comparative analysis of different cases of spatial and temporal star pair separations.

An estimate of the standard deviation of the single axis star position measurement error,  $\sigma_0$ , for star tracker measurements (Reference 1) and the standard deviation of the single axis IMU bias drift rate,  $\sigma_d$ , (Appendix A) are given by

$$\sigma_0 = 71.5 \widehat{\text{sec}}$$

$$\sigma_d = 0.02 \widehat{\text{sec/sec}}$$

These performance estimates in conjunction with equation 10 were used to compute the analytical estimates of the RMS IMU alignment error for the 18 cases of spatial and temporal star pair separations listed in Table 4.1-1. In

TABLE 4.1-1 RMS TOTAL IMU ALIGNMENT ERROR

Case	$\delta$	t	RMS ALIGNMENT ERROR ( $\widehat{\text{sec}}$ )		
			Analytical Estimate	Monte Carlo Result	Curve Fit
1	90	0	124	121	118
2	90	30	129	130	124
3	90	60	143	148	139
4	90	90	164	163	160
5	75	15	128	121	123
6	75	45	139	141	134
7	75	75	157	159	153
8	60	0	137	131	131
9	60	30	143	131	137
10	60	60	160	165	155
11	60	90	185	184	181
12	45	15	162	147	155
13	45	45	177	171	171
14	45	75	204	193	199
15	30	0	215	188	205
16	30	30	226	193	217
17	30	60	258	250	251
18	30	90	304	300	298

order to validate this model, also included in the table are the IMUCAL simulation derived values of the RMS alignment error. Note that the analytical estimates compare very well with the Monte Carlo simulation results. This verifies that the model (equation 10), used for estimating the alignment error is a valid model. There is, therefore, a high degree of confidence in this model based on both this verification and the original, rigorous development of the model. Conversely, many simplifying assumptions were made to approximate the star sighting error,  $\sigma_0$ ; therefore, there is still some uncertainty in the estimated value. In order to determine a more accurate estimate of  $\sigma_0$ , a curve fit to the simulation results was made using equation 10 and the known standard deviation of the simulated IMU drift rate (0.02 sec/sec). The results of the curve fit yields the following value for  $\sigma_0$ :

$$\sigma_0 = 68.4 \text{ sec}$$

This value compares favorably with the estimated value. Table 4.1-1 contains data for the best fit surface to the simulation results using this empirically derived value for  $\sigma_0$ . The RMS IMU alignment error (equation 10) is plotted in Figure 4.1-1 as a function of the spatial and temporal star pair separations using the simulation derived value of  $\sigma_0$ . On this plot, there are several time scales corresponding to different values of the standard deviation in the single axis IMU drift rate,  $\sigma_d$ .

#### 4.2 THE SINGLE AXIS IMU ALIGNMENT ERROR

For the purpose of navigation analysis, it is often desired to know the alignment accuracy with respect to the individual axes of an inertial coordinate system. The single-axis alignment error properties, defined by equations D-4 and D-5, in Appendix D, apply only when the error vector  $\phi$  is resolved into the star pair relative coordinate system. The star pair coordinate system, however, can assume any orientation with respect to either the Mean-of-1950 coordinate system or the IMU platform coordinate system. If the orientation of the star pair coordinate system is assumed to be uniformly random in three-space, the alignment error will be isotropic in an inertial reference coordinate system. The distributions of the components, however, will not in general be Gaussian and, furthermore, cannot be solved for in closed form. Two important properties of this distribution can be inferred from the symmetry of the star pair coordinate system components and the uniformity of the coordinate system's random orientation:

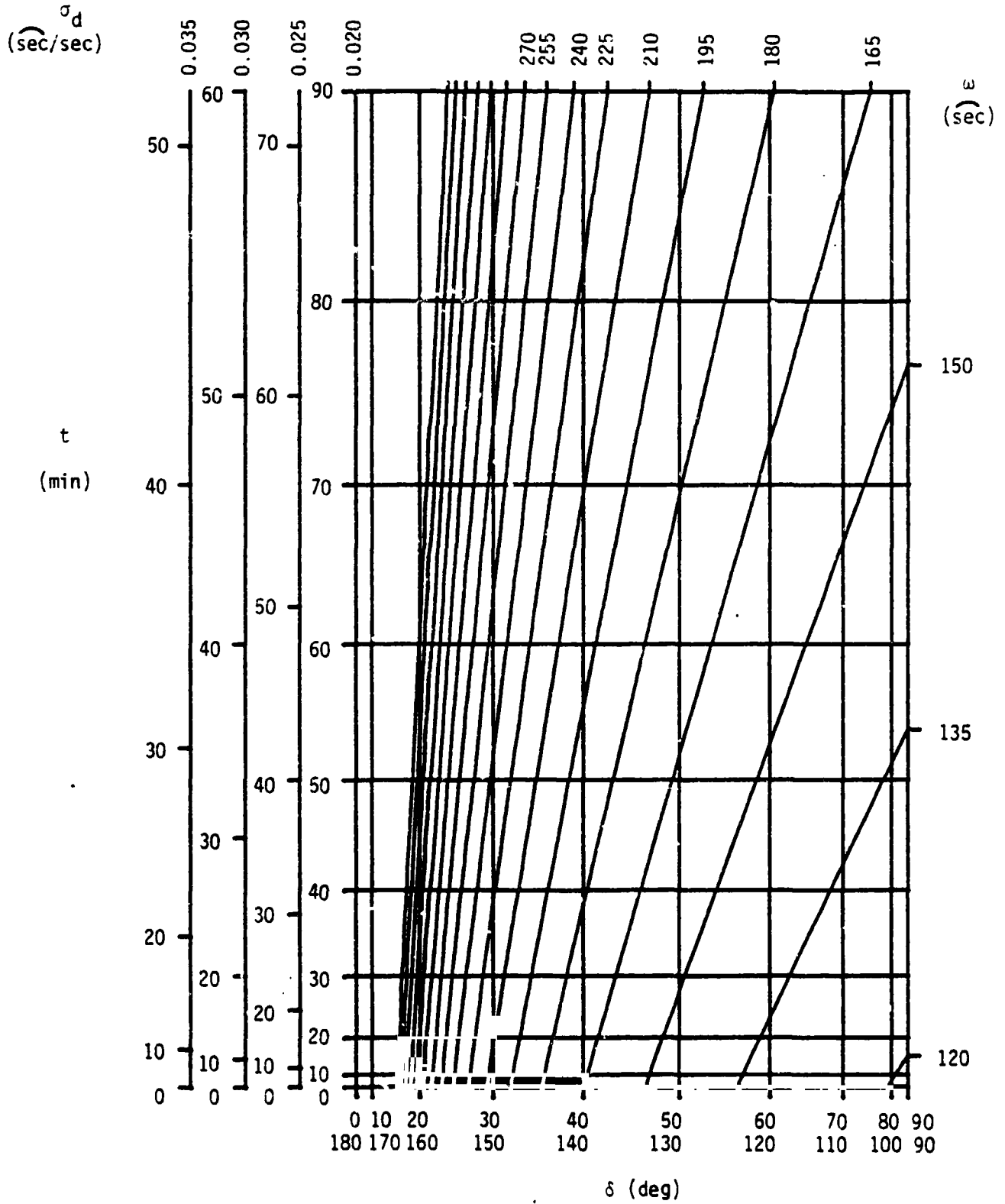
$$\mu_x = \mu_y = \mu_z = 0, \text{ and} \quad (11)$$

$$\sigma_x = \sigma_y = \sigma_z = \omega_0. \quad (12)$$

The subscripts x, y, and z are redefined to denote the coordinate axes of the inertial reference coordinate system. The equation for the RMS IMU alignment error (equation D-12) is valid for any coordinate system; therefore, equations D-12 and 12 can be combined to yield a solution for the variance of the single-axis IMU alignment error.

$$\omega_0^2 = \omega^2/3 \quad (13)$$

FIGURE 4.1-1 RMS IMU ALIGNMENT ERROR



The standard deviation of the single axis IMU alignment error is plotted as a function of the spatial and temporal star pair separations in Figure 4.2-1. The empirically derived value for  $\sigma_0$  was used to generate the plot. There are several time scales corresponding to different values of the standard deviation in the single-axis IMU drift rate.

The assumption concerning the isotropic nature of the IMU alignment error in the IMU platform coordinate system requires closer examination. The total alignment error is a vector sum of all the system measurement error components. Each error component has an associated direction that is determined by the relative orientation of the star tracker sensor measurement plane with respect to the IMU platform. Since the IMU platform was initialized at a random position in each Monte Carlo cycle, the distributions of the error components are expected to be isotropic. To test this assumption, an error covariance matrix was computed for the STS-1 case (manual ST mode), using all 300 samples (that is, data from the 3 IMU's for Case 1):

$$C = \begin{bmatrix} 4369 & 161 & 229 \\ 161 & 4416 & 60 \\ 229 & 60 & 5251 \end{bmatrix} \quad (14)$$

This covariance matrix is expressed in the IMU platform coordinate system and the units of the elements are  $\text{sec}^2$ . The covariance matrix defines an error ellipsoid by the equation

$$K^2 = [X \ Y \ Z] C^{-1} \begin{bmatrix} X \\ Y \\ Z \end{bmatrix} \quad (15)$$

The probability that an alignment error sample  $\phi_i$  will be inside the ellipsoid is a function of the parameter K. The lengths of the principal axes of the ellipsoid are given by

$$\sigma_{\bar{x}} K = 73 K \widehat{\text{sec}}$$

$$\sigma_{\bar{y}} K = 67 K \widehat{\text{sec}}$$

$$\sigma_{\bar{z}} K = 65 K \widehat{\text{sec}}$$

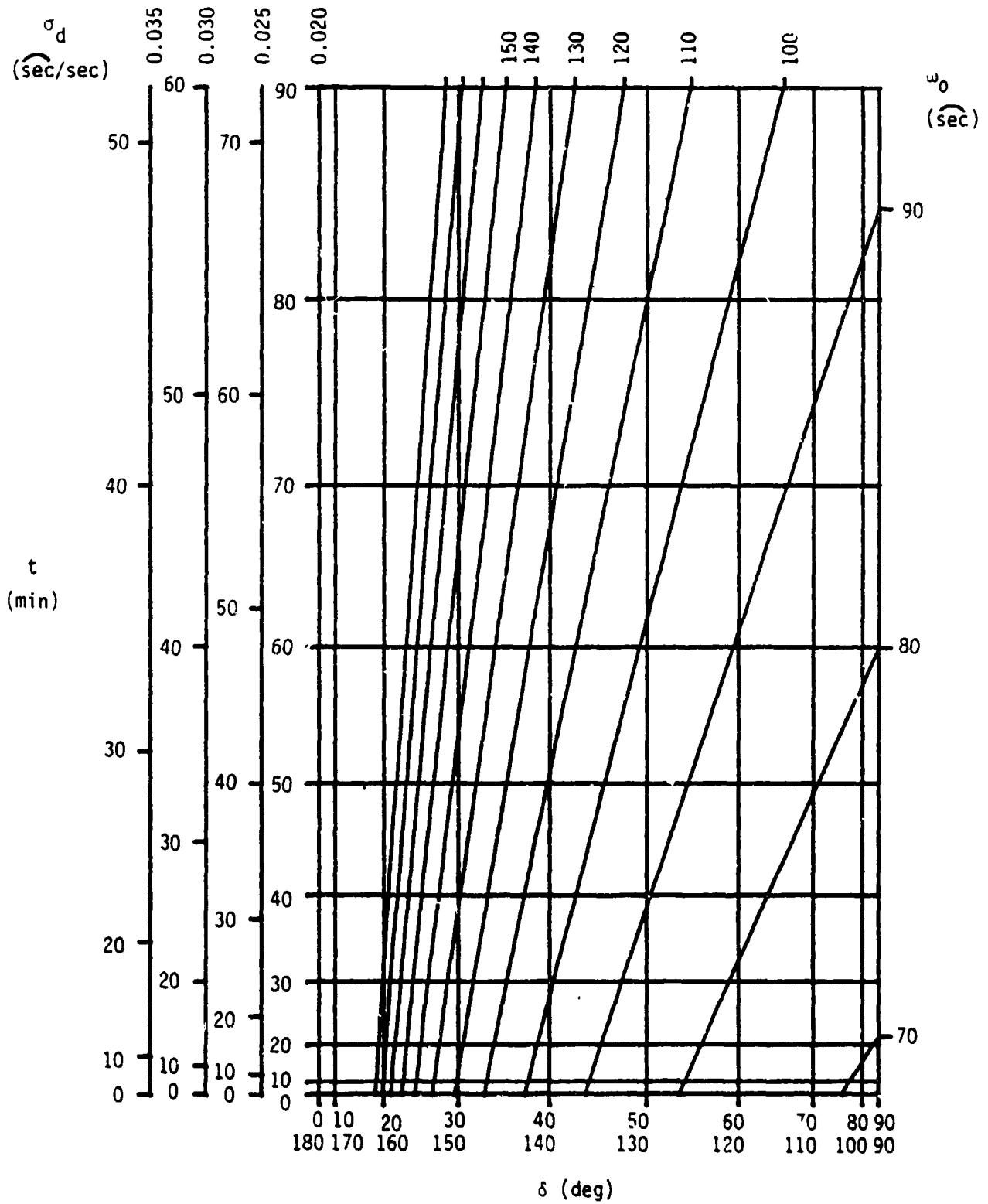
Since the probability ellipsoid approximates a sphere, the assumption of equal single-axis variances is reasonable.

$$\sigma_{\bar{x}}^2 = \sigma_{\bar{y}}^2 = \sigma_{\bar{z}}^2 = \omega_0^2 \quad (16)$$

The equation of the probability ellipsoid (equation 15), therefore, simplifies to that of a sphere with radius  $\omega_0 K$ .

$$(\omega_0 K)^2 = X^2 + Y^2 + Z^2 \quad (17)$$

FIGURE 4.2-1  
STANDARD DEVIATION OF THE SINGLE AXIS IMU ALIGNMENT ERROR





Note that the semiaxis ( $\sigma_x K$ ), which is approximately parallel to the Z platform axis, is slightly longer than the other semiaxes. Covariance matrix diagonal elements were computed for the remaining 17 cases (using all 300 samples as in case 1) and, in all but one case (case 18), the variance in the Z-axis error was slightly larger than the variance in both the X- and Y-axis error. The variance in the X- and Y-axis errors were approximately equal in each case. This characteristic is a result of the choice of coordinate system. The azimuth resolver measurement error is not isotropic, but is unique since it is always parallel to the Z platform axis. The alignment error ellipsoid, therefore, is slightly elongated in the direction of the azimuth platform axis. For navigation simulations using the comprehensive IMU hardware model described in the Onboard Navigation Systems Characteristics document, the following values of the one sigma IMU alignment errors about the platform axes for STS-1 alignments ( $\delta = 90^\circ$  &  $t = 0$ ) are recommended:

$$\sigma_x = 66 \widehat{\text{sec}}$$

$$\sigma_y = 66 \widehat{\text{sec}}$$

$$\sigma_z = 72 \widehat{\text{sec}}$$

#### 4.3 THE MAXIMUM EXPECTED IMU ALIGNMENT ERROR

It is often useful to know the range of the alignment error magnitude. Worst case is usually assumed to be three standard deviations from the mean for single dimensional random variables. There is a 99.74% probability that the single dimensional normally distributed random variable  $W$  is within three standard deviations of the mean.

$$P(\mu - 3\sigma < W < \mu + 3\sigma) = 0.9974$$

In the three dimensional case, the range associated with a given probability is an ellipsoidal volume centered about the mean. The mean IMU alignment error is zero for all three platform axes (equation 11) and the range is approximated by a spherical volume of radius  $\omega_0 K$  (equation 17). The probability that an alignment error sample is contained within this volume is a function of the distribution and the value of  $K$ . A worst case IMU alignment error sample is defined to have a length that is equal to the radius of a sphere that encompasses 99.74% of the population of alignment error samples. If the alignment error  $\phi$  is assumed normally distributed\*, then the value of  $K$  for this sphere is 3.77.

---

\* The IMU alignment error is normally distributed only in the STS-1 (manual ST mode) case ( $\delta = 90^\circ$  &  $t = 0$  min). It has been shown, however, that the actual distribution for the general case closely approximates the normal distribution for the entire range of star pair temporal separations and a limited range of spatial separations.

$$60^\circ < \delta < 120^\circ$$

$$0 \text{ min} < t < 90 \text{ min}$$

$$P(|\phi| < 3.77 \omega_0) = 0.9974 \quad (18)$$

Therefore,

$$|\phi|_{\max} = 3.77 \omega_0 \quad (19)$$

Note that the worst case error is a total error and that the single axis components will be smaller. Lines of constant maximum IMU alignment error (equation 19) are plotted as a function of the star pair temporal and spatial separations in Figure 4.3-1. In spite of the assumptions made, the estimated maximum IMU alignment error as defined by equation 19 compares favorably with the simulation results in Appendix B.

#### 4.4 THE STS-1 CASE

The following summarizes the statistics for the STS-1 type (manual ST mode) alignments (see Table 4.0-1 for nomenclature). Derivation of these statistics is presented in Appendix D.

$$\mu_x = \mu_y = \mu_z = 0$$

$$\sigma_x = \sigma_y = \sigma_z = 68 \widehat{\text{sec}}$$

$$\mu = 109 \widehat{\text{sec}}$$

$$\sigma = 46 \widehat{\text{sec}}$$

$$\omega = 118 \widehat{\text{sec}}$$

$$\omega_0 = 68 \widehat{\text{sec}}$$

$$|\phi|_{\max} = 258 \widehat{\text{sec}}$$

#### 4.5 SPECIAL CASES

The eighteen test cases in Table 4.1-1 simulated star pair separations that were less than or equal to 90 degrees. These cases were limited to this range because of the symmetry of the alignment error function (equation 10) with respect to 90 degrees. An additional case, however, was simulated to verify the property of symmetry. Table 4.5-1 summarizes the results of this case.

FIGURE 4.3-1  
ESTIMATED MAXIMUM TOTAL IMU ALIGNMENT ERROR

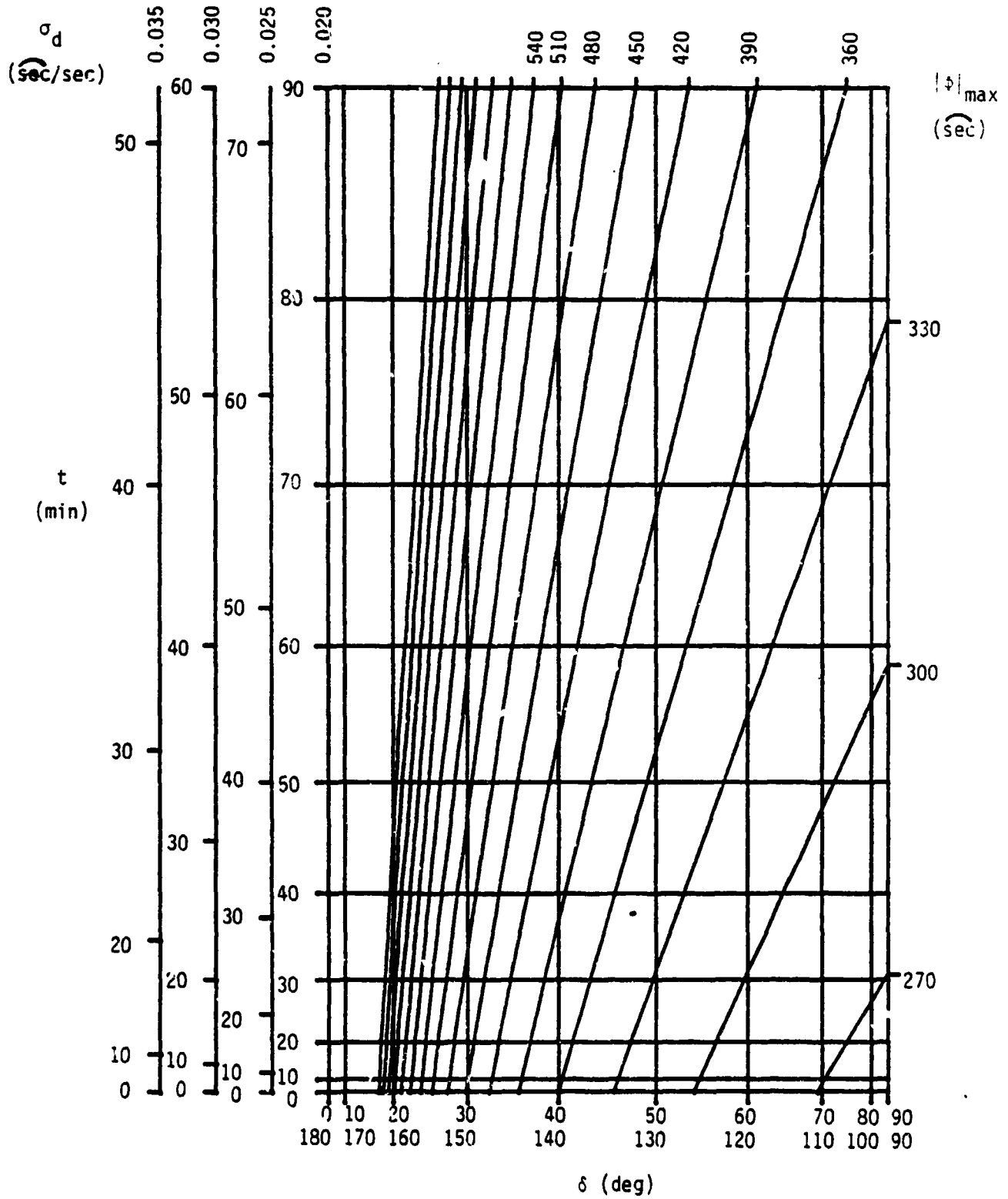


TABLE 4.5-1 RMS ALIGNMENT ERROR - SPECIAL CASES

			RMS ALIGNMENT ERROR ( $\widehat{\text{sec}}$ )		
Case	$\delta$	t	Analytical Estimate	Monte Carlo Result	Curve Fit
$\delta > 90^\circ$	150	60	258	241	251
post-sleep	90	0	124	125	118

One final case was simulated to assess the feasibility of star acquisition with large amounts of IMU drift. The longest period between alignments for STS-1 will occur during the crew sleep periods. The first post-sleep alignment for STS-1 was simulated for 200 Monte Carlo cycles. This alignment occurs ten hours and thirty minutes after the previous alignment. As in the other cases, the standard deviation in the per axis IMU drift rate was 0.02 degrees per hour. In the 200 attempts to acquire both stars in the offset mode, 28 failed. This corresponds to an 86% probability of success for offset mode acquisition when performing post-sleep alignments. This probability is based on the simulation of a perfect star tracker and a celestial sphere devoid of everything but navigation stars. Hardware anomalies and non-navigation trackable objects would decrease this estimate slightly for actual flight. The simulation was configured to investigate acquisition probability for only the offset mode. When the desired star is not found in the offset mode, the tracker is commanded to search the full field of view. The simulation program, however, cannot be used to determine the acquisition probability for full field search mode because of uncertainties in debris density and angular rates.

## 5.0 CONCLUSIONS AND RECOMMENDATIONS

In summary, the orbit IMU alignment accuracy analysis results compare favorably with previous estimates. The simulation-derived value for the standard deviation in the single-axis IMU alignment error ( $\omega_0$ ) for STS-1 alignments is 68 arc seconds. This corresponds to a 99.7% probability that the magnitude of the total alignment error is less than 258 arc seconds. The simulation program also verified the analytic algorithm for estimating the IMU alignment accuracy (equation 10) as a function of the spatial and temporal separation of measured star pairs.

### 5.1 CREW PROCEDURES

Based upon this analysis, several recommendations concerning crew procedures for IMU alignments are made. Before the IMU platform is repositioned, the crew will check the displayed IMU torquing angles for reasonableness. If the angles are less than an acceptable limit, then the repositioning of the IMU platforms is executed, otherwise, the star measurements must be repeated. The torquing angle limit must be sized to include the initial alignment error, the IMU drift error since the initial alignment, and the final alignment error. The longest intervals between alignments are during the crew sleep periods and can be as long as 10.5 hours for STS-1. The variance in the torquing angles, therefore, is

$$\sigma_{\tau}^2 = \omega_0^2 + (10.5 \sigma_d)^2 + \omega_0^2$$
$$\sigma_{\tau} = 762 \widehat{\text{sec}}$$

The maximum expected magnitude of the torquing vector  $\tau$  is defined by

$$P(|\tau| < 3.77 \sigma_{\tau}) = 0.9974$$

$$|\tau|_{\text{max}} = 0.8^{\circ}$$

For simplicity, present crew procedures require that the largest torquing angle component be less than the acceptable limit; therefore, the recommended torquing angle limit criteria for alignment is

$$\tau_x < 0.8^{\circ}$$

$$\tau_y < 0.8^{\circ}$$

$$\tau_z < 0.8^{\circ}$$

This recommended value confirms the value currently in the STS-1 crew procedures. This simplified torquing angle component test is crude and not as exact as a magnitude ( $|\tau|$ ) test. This could be resolved by displaying  $|\tau|$  on the IMU alignment display. The torquing vector magnitude is presently available in the flight software as the variable CGMV\_QANG in the procedure GX1\_MIS\_ANG.

The displayed torquing angles are also crew evaluated during IMU alignment verification. After each STS-1 alignment, a second alignment is performed

to verify the first. If any one of the displayed verification torquing angles exceeds an acceptable limit, then the alignment and verification process must be repeated. The verification torquing angle limit must be sized to include the initial IMU alignment error and the verification alignment error. The variance in the verification angles will be

$$\sigma_{\tau}^2 = \omega_0^2 + \omega_0^2$$

$$\sigma_{\tau} = 97 \widehat{\text{sec}}$$

The maximum expected magnitude of the verification torquing vector  $\tau$  is defined by

$$P(|\tau| < 3.77 \sigma_{\tau}) = 0.9974$$

$$|\tau|_{\text{max}} = 0.1^{\circ}$$

As in the alignment case, the crew performs a rough check by simply verifying that each torquing angle component is less than the torquing angle limit. The recommended verification criteria, therefore, is

$$\tau_x < 0.1^{\circ}$$

$$\tau_y < 0.1^{\circ}$$

$$\tau_z < 0.1^{\circ}$$

Again, this recommended value confirms the value currently in the STS-1 crew procedures.

## 6.0 REFERENCES

1. Corson, R. W., "ONORBIT IMU ALIGNMENT ERROR BUDGET", JSC Internal Note No. 80-FM-17, March 1980.
2. Corson, R. W., "ORBIT IMU ALIGNMENT - Interpretation of Onboard Display Data", JSC Internal Note No. 78-FM-34, June 1978.

APPENDIX A  
STAR TRACKER, IMU, AND NAV BASE  
ERROR MODEL PARAMETERS



### IMU ERROR MODEL

Error Source	$1\sigma$ per axis error (arc sec)
Resolver errors	
Resolver bias	30
Random noise	12
Quantization	11.5
Sinusoidal bias	
1st harmonic	7.6
8th harmonic	19.0
9th harmonic	4.2
16th harmonic	20.0
Gimbal nonorthogonalities	
Pitch-to-outer roll	30
Outer roll to case	20
Gyro errors	
Bias drift	.02/sec

### NAV BASE ERROR MODEL

Error Source	$1\sigma$ per axis error (arc sec)
IMU LRU installation	20
Thermal nav base bending (ST to IMU)	13.7
IMU to ST structural uncertainty	7.1
ST LRU installation	20

### STAR TRACKER ERROR MODEL

Error Source	$1\sigma$ per axis error (arc sec)
Bias	42.4
Random	10.6

APPENDIX B  
MONTE CARLO SIMULATION DERIVED  
IMU ALIGNMENT ERROR STATISTICS

TABLE B-1 KEY TO SIMULATION PROGRAM OUTPUTS

IMU ALIGNMENT ERROR IN ARC SECONDS	$\delta \times t$									K SAMPLES			
	IMU 1			IMU 2			IMU 3				IMU 1	IMU 2	IMU 3
	X	Y	Z	X	Y	Z	X	Y	Z	RSS	RSS	RSS	RSS
MEAN $(\phi_x)_1$	$(\mu_x)_1$	$(\mu_y)_1$	$(\mu_z)_1$	$(\mu_x)_2$	$(\mu_y)_2$	$(\mu_z)_2$	$(\mu_x)_3$	$(\mu_y)_3$	$(\mu_z)_3$	$(\mu)_1$	$(\mu)_2$	$(\mu)_3$	$(\mu)_{123}$
SIGMA $(\sigma_x)_1$	$(\sigma_x)_1$	$(\sigma_y)_1$	$(\sigma_z)_1$	$(\sigma_x)_2$	$(\sigma_y)_2$	$(\sigma_z)_2$	$(\sigma_x)_3$	$(\sigma_y)_3$	$(\sigma_z)_3$	$(\sigma)_1$	$(\sigma)_2$	$(\sigma)_3$	$(\sigma)_{123}$
RMS $(\omega_0)_1$	$(\omega_0)_1$	$(\omega_0)_1$	$(\omega_0)_1$	$(\omega_0)_2$	$(\omega_0)_2$	$(\omega_0)_2$	$(\omega_0)_3$	$(\omega_0)_3$	$(\omega_0)_3$	$(\omega)_1$	$(\omega)_2$	$(\omega)_3$	$(\omega)_{123}$
MAX $\max(\phi_x)_1$	$\max(\phi_x)_1$	$\max(\phi_y)_1$	$\max(\phi_z)_1$	$\max(\phi_x)_2$	$\max(\phi_y)_2$	$\max(\phi_z)_2$	$\max(\phi_x)_3$	$\max(\phi_y)_3$	$\max(\phi_z)_3$	$\max( \phi )_1$	$\max( \phi )_2$	$\max( \phi )_3$	$\max( \phi )_{123}$
MIN $\min(\phi_x)_1$	$\min(\phi_x)_1$	$\min(\phi_y)_1$	$\min(\phi_z)_1$	$\min(\phi_x)_2$	$\min(\phi_y)_2$	$\min(\phi_z)_2$	$\min(\phi_x)_3$	$\min(\phi_y)_3$	$\min(\phi_z)_3$	$\min( \phi )_1$	$\min( \phi )_2$	$\min( \phi )_3$	$\min( \phi )_{123}$

where:

$$(\phi_j)_n = \frac{1}{k} \sum_{i=1}^k ((\phi_j)_n)_i$$

$$(\sigma_j)_n = \sqrt{\frac{1}{k-1} \left[ \sum_{i=1}^k ((\phi_j)_n)_i^2 - \frac{1}{k} \left( \sum_{i=1}^k ((\phi_j)_n)_i \right)^2 \right]}$$

$$(\mu)_n = \frac{1}{k} \sum_{i=1}^k (|\phi|)_n)_i$$

$$(\sigma)_n = \sqrt{\frac{1}{k-1} \left[ \sum_{i=1}^k (|\phi|)_n)_i^2 - \frac{1}{k} \left( \sum_{i=1}^k (|\phi|)_n)_i \right)^2 \right]}$$

$$(\omega)_n = \sqrt{(\mu^2 + (\sigma)^2)_n} = \sqrt{(\sigma_x)_n^2 + (\sigma_y)_n^2 + (\sigma_z)_n^2} = \sqrt{3} (\omega_0)_n$$

J = x, y, z n = 1, 2, 3

$\delta$  = spatial separation in degrees

t = temporal separation in minutes

TABLE B-2 IMU ALIGNMENT ERROR STATISTICS FOR 90° STAR PAIR ANGULAR SEPARATIONS

IMU ALIGNMENT ERROR IN ARC SECONDS		CASE 1			90° x 0 min			100 SAMPLES			
		IMU 2			IMU 3			IMU 1	IMU 2	IMU 3	ALL
MEAN	SIGMA	X	Y	Z	X	Y	Z	RSS	RSS	RSS	RSS
1.	03.	-2.	-0.	-3.	-6.	-0.	-5.	112.	119.	104.	112.
69.	63.	99.	72.	97.	66.	69.	68.	43.	47.	44.	49.
69.	69.	74.	74.	71.	74.	67.	67.	120.	120.	114.	121.
173.	101.	184.	174.	203.	177.	183.	174.	190.	241.	235.	241.
-193.	-155.	-139.	-166.	-174.	-166.	-140.	-150.	23.	59.	59.	23.

IMU ALIGNMENT ERROR IN ARC SECONDS		CASE 2			90° x 30 min			100 SAMPLES			
		IMU 2			IMU 3			IMU 1	IMU 2	IMU 3	ALL
MEAN	SIGMA	X	Y	Z	X	Y	Z	RSS	RSS	RSS	RSS
-14.	7.	12.	3.	-11.	-4.	-9.	-1.	121.	117.	110.	119.
76.	72.	71.	99.	79.	68.	68.	62.	60.	49.	49.	53.
78.	70.	59.	93.	59.	74.	74.	74.	135.	127.	128.	130.
193.	224.	244.	193.	196.	146.	216.	299.	302.	249.	311.	311.
-213.	-194.	-172.	-172.	-201.	-136.	-126.	-227.	14.	16.	17.	14.

IMU ALIGNMENT ERROR IN ARC SECONDS		CASE 3			90° x 60 min			100 SAMPLES			
		IMU 2			IMU 3			IMU 1	IMU 2	IMU 3	ALL
MEAN	SIGMA	X	Y	Z	X	Y	Z	RSS	RSS	RSS	RSS
0.	10.	3.	23.	0.	11.	-9.	7.	136.	135.	134.	135.
74.	77.	74.	96.	90.	90.	76.	94.	50.	55.	66.	60.
85.	85.	84.	84.	84.	86.	86.	86.	140.	146.	149.	148.
140.	107.	219.	243.	200.	226.	167.	325.	270.	204.	369.	369.
-172.	-206.	-101.	-150.	-240.	-211.	-197.	-197.	30.	37.	29.	29.

IMU ALIGNMENT ERROR IN ARC SECONDS		CASE 4			90° x 90 min			98 SAMPLES			
		IMU 2			IMU 3			IMU 1	IMU 2	IMU 3	ALL
MEAN	SIGMA	X	Y	Z	X	Y	Z	RSS	RSS	RSS	RSS
-3.	12.	14.	11.	10.	-4.	3.	13.	147.	144.	151.	147.
91.	91.	94.	94.	94.	97.	93.	107.	60.	74.	79.	79.
93.	93.	94.	94.	94.	96.	96.	93.	101.	162.	167.	153.
192.	224.	305.	243.	290.	239.	105.	300.	331.	430.	302.	430.
-102.	-223.	-323.	-193.	-201.	-309.	-160.	-310.	40.	23.	21.	21.

TABLE B-3 IMU ALIGNMENT ERROR STATISTICS FOR 75° STAR PAIR ANGULAR SEPARATIONS

IMU ALIGNMENT ERROR IN ARC SECONDS		75° x 15 min								
		CASE 5			CASE 6			CASE 7		
		IMU 1			IMU 2			IMU 3		
		X	Y	Z	X	Y	Z	X	Y	Z
MEAN		4.	17.	-1.	15.	6.	4.	-0.	7.	5.
SIGMA		64.	65.	74.	70.	69.	60.	65.	71.	01.
RMS		60.	60.	60.	69.	60.	69.	73.	71.	71.
MAX		153.	100.	137.	287.	174.	170.	150.	187.	259.
MIN		-130.	-130.	-219.	-140.	-151.	-101.	-144.	-167.	-145.
		IMU 1			IMU 2			IMU 3		
		RSS	RSS	RSS	RSS	RSS	RSS	RSS	RSS	RSS
		109.	110.	110.	109.	110.	110.	109.	110.	111.
		46.	49.	49.	46.	49.	49.	46.	49.	50.
		110.	120.	120.	110.	120.	120.	110.	120.	121.
		240.	302.	302.	240.	302.	302.	240.	302.	302.
		14.	12.	12.	14.	12.	12.	14.	12.	12.
		IMU 1			IMU 2			IMU 3		
		RSS	RSS	RSS	RSS	RSS	RSS	RSS	RSS	RSS
		131.	124.	124.	131.	124.	124.	131.	124.	128.
		66.	57.	57.	66.	57.	57.	66.	57.	60.
		147.	136.	136.	147.	136.	136.	147.	136.	147.
		350.	289.	289.	350.	289.	289.	350.	289.	353.
		20.	15.	15.	20.	15.	15.	20.	15.	6.
		IMU 1			IMU 2			IMU 3		
		RSS	RSS	RSS	RSS	RSS	RSS	RSS	RSS	RSS
		149.	130.	130.	149.	130.	130.	149.	130.	144.
		67.	73.	73.	67.	73.	73.	67.	73.	67.
		163.	157.	157.	163.	157.	157.	163.	157.	159.
		331.	310.	310.	331.	310.	310.	331.	310.	339.
		30.	20.	20.	30.	20.	20.	30.	20.	20.

TABLE B-4 IMU ALIGNMENT ERROR STATISTICS FOR 60° STAR PAIR ANGULAR SEPARATIONS

IMU ALIGNMENT ERROR IN ARC SECONDS		CASE 8			60° x 0min			100 SAMPLES			
		IMU 2			IMU 3			IMU 1	IMU 2	IMU 3	ALL
		X	Y	Z	X	Y	Z	RSS	RSS	RSS	RSS
MEAN		2.	-2.	-15.	9.	-12.	-16.	120.	122.	115.	119.
SIGMA		75.	75.	84.	79.	97.	94.	62.	54.	50.	55.
RMS		70.	70.	70.	77.	77.	72.	133.	133.	125.	131.
MAX		205.	250.	216.	170.	105.	142.	290.	205.	251.	290.
MIN		-269.	-239.	-223.	-253.	-103.	-207.	31.	21.	31.	21.

IMU ALIGNMENT ERROR IN ARC SECONDS		CASE 9			60° x 30 min			100 SAMPLES			
		IMU 2			IMU 3			IMU 1	IMU 2	IMU 3	ALL
		X	Y	Z	X	Y	Z	RSS	RSS	RSS	RSS
MEAN		0.	9.	-20.	3.	-4.	4.	125.	122.	111.	119.
SIGMA		71.	82.	81.	80.	83.	80.	54.	58.	47.	54.
RMS		79.	79.	79.	78.	78.	70.	137.	133.	120.	131.
MAX		255.	264.	205.	227.	143.	280.	330.	362.	266.	362.
MIN		-173.	-247.	-223.	-203.	-159.	-163.	31.	20.	30.	20.

IMU ALIGNMENT ERROR IN ARC SECONDS		CASE 10			60° x 60 min			100 SAMPLES			
		IMU 2			IMU 3			IMU 1	IMU 2	IMU 3	ALL
		X	Y	Z	X	Y	Z	RSS	RSS	RSS	RSS
MEAN		-4.	7.	7.	1.	20.	-1.	152.	149.	145.	149.
SIGMA		92.	85.	100.	80.	102.	97.	71.	66.	75.	70.
RMS		97.	97.	97.	94.	94.	94.	160.	163.	163.	163.
MAX		194.	103.	300.	165.	347.	250.	310.	347.	459.	459.
MIN		-232.	-270.	-200.	-183.	-179.	-201.	47.	31.	32.	31.

IMU ALIGNMENT ERROR IN ARC SECONDS		CASE 11			60° x 90 min			100 SAMPLES			
		IMU 2			IMU 3			IMU 1	IMU 2	IMU 3	ALL
		X	Y	Z	X	Y	Z	RSS	RSS	RSS	RSS
MEAN		7.	-3.	6.	14.	15.	-2.	173.	151.	167.	164.
SIGMA		100.	111.	120.	103.	97.	97.	90.	82.	87.	84.
RMS		110.	110.	110.	88.	89.	86.	191.	172.	188.	184.
MAX		303.	270.	337.	335.	404.	230.	464.	469.	570.	570.
MIN		-106.	-419.	-223.	-223.	-223.	-203.	23.	15.	36.	15.



TABLE B-6 IMU ALIGNMENT ERROR STATISTICS FOR 30° STAR PAIR ANGULAR SEPARATIONS

IMU ALIGNMENT ERROR IN ARC SECONDS		CASE 15									100 SAMPLES			
		IMU 1			IMU 2			IMU 3			IMU 1	IMU 2	IMU 3	ALL
		X	Y	Z	X	Y	Z	X	Y	Z	RSS	RSS	RSS	RSS
MEAN		0.	-16.	-7.	-5.	-5.	-10.	-3.	-6.	-20.	161.	160.	171.	164.
SIGMA		06.	127.	99.	126.	126.	97.	101.	95.	142.	86.	85.	102.	91.
RMS		105.	105.	105.	105.	105.	105.	115.	115.	115.	183.	182.	199.	188.
MAX		342.	265.	104.	300.	300.	313.	203.	204.	407.	402.	420.	451.	451.
MIN		-184.	-367.	-297.	-207.	-207.	-201.	-206.	-232.	-346.	46.	36.	17.	17.

IMU ALIGNMENT ERROR IN ARC SECONDS		CASE 16									100 SAMPLES			
		IMU 1			IMU 2			IMU 3			IMU 1	IMU 2	IMU 3	ALL
		X	Y	Z	X	Y	Z	X	Y	Z	RSS	RSS	RSS	RSS
MEAN		3.	9.	-34.	12.	-9.	-11.	-2.	9.	5.	175.	171.	157.	168.
SIGMA		99.	109.	135.	109.	126.	112.	116.	96.	90.	102.	104.	177.	95.
RMS		117.	117.	116.	116.	116.	116.	101.	101.	101.	202.	200.	175.	193.
MAX		353.	302.	271.	367.	362.	300.	304.	293.	249.	461.	490.	373.	490.
MIN		-244.	-363.	-306.	-587.	-36.	211.	343.	-276.	-264.	20.	12.	5.	5.

IMU ALIGNMENT ERROR IN ARC SECONDS		CASE 17									100 SAMPLES			
		IMU 1			IMU 2			IMU 3			IMU 1	IMU 2	IMU 3	ALL
		X	Y	Z	X	Y	Z	X	Y	Z	RSS	RSS	RSS	RSS
MEAN		-5.	7.	26.	7.	39.	-1.	26.	-17.	1.	215.	220.	213.	216.
SIGMA		127.	144.	159.	127.	169.	134.	142.	133.	153.	166.	124.	131.	127.
RMS		144.	144.	144.	144.	144.	144.	144.	144.	144.	250.	252.	250.	250.
MAX		324.	423.	424.	409.	390.	359.	451.	350.	774.	675.	616.	851.	851.
MIN		-350.	-579.	-439.	-333.	-296.	-375.	-606.	-334.	-412.	44.	31.	14.	14.

IMU ALIGNMENT ERROR IN ARC SECONDS		CASE 18									100 SAMPLES			
		IMU 1			IMU 2			IMU 3			IMU 1	IMU 2	IMU 3	ALL
		X	Y	Z	X	Y	Z	X	Y	Z	RSS	RSS	RSS	RSS
MEAN		-7.	9.	-0.	29.	-12.	-10.	-9.	-13.	-20.	222.	257.	272.	250.
SIGMA		162.	164.	164.	170.	175.	152.	204.	170.	207.	195.	141.	207.	162.
RMS		150.	150.	150.	169.	169.	169.	169.	169.	169.	200.	20.	202.	304.
MAX		571.	507.	321.	912.	516.	365.	727.	450.	470.	777.	633.	690.	694.
MIN		-674.	-703.	-470.	-405.	-550.	-471.	-604.	-553.	-652.	20.	31.	17.	17.



APPENDIX C  
TOTAL AND SINGLE-AXIS IMU  
ALIGNMENT ERROR PROBABILITY  
DENSITY FUNCTIONS FOR STS-1  
TYPE ALIGNMENTS

FIGURE C-1 TOTAL IMU ALIGNMENT ERROR PROBABILITY DENSITY FUNCTION

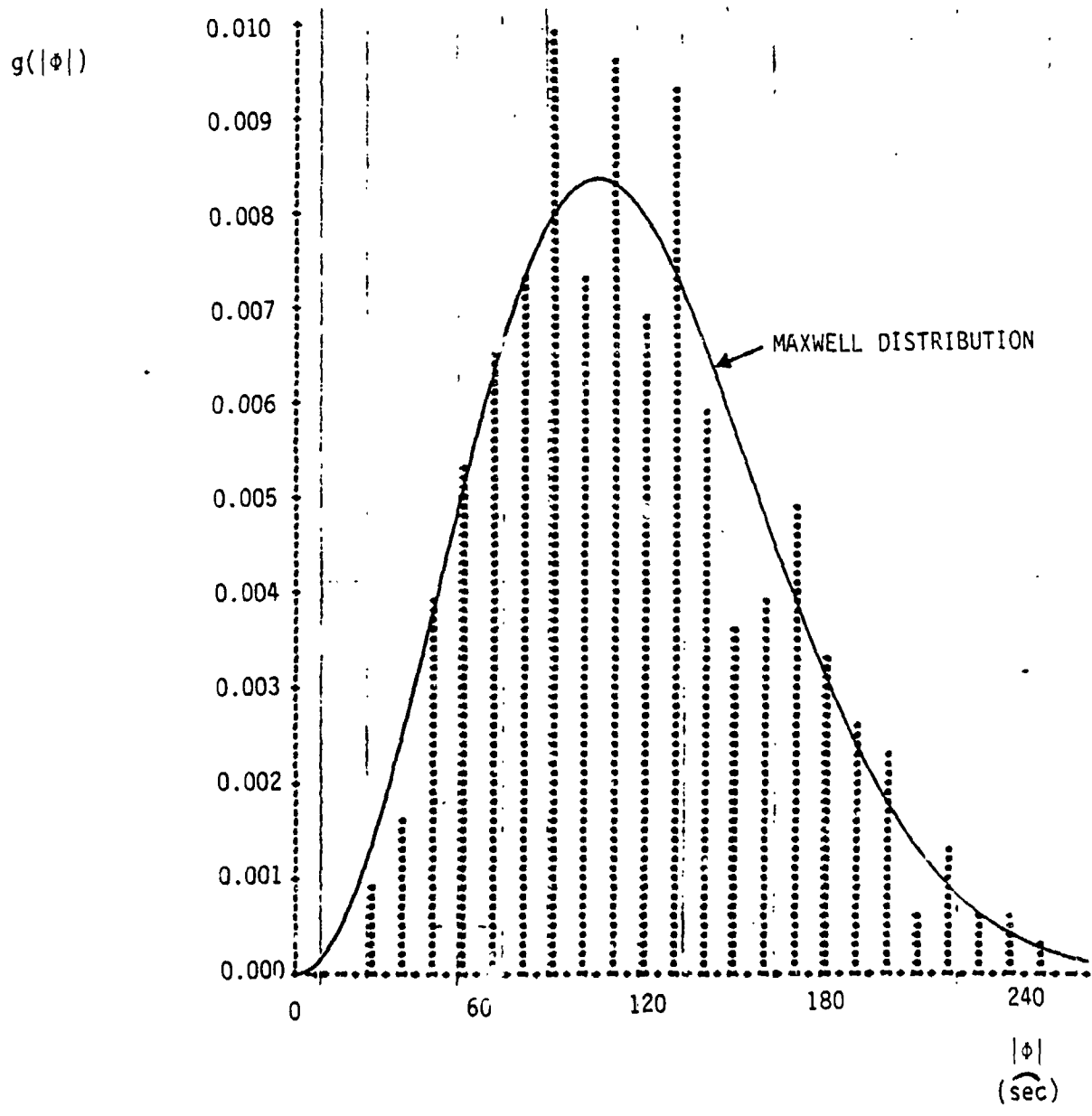


FIGURE C-2 X-AXIS IMU ALIGNMENT ERROR  
PROBABILITY DENSITY FUNCTION

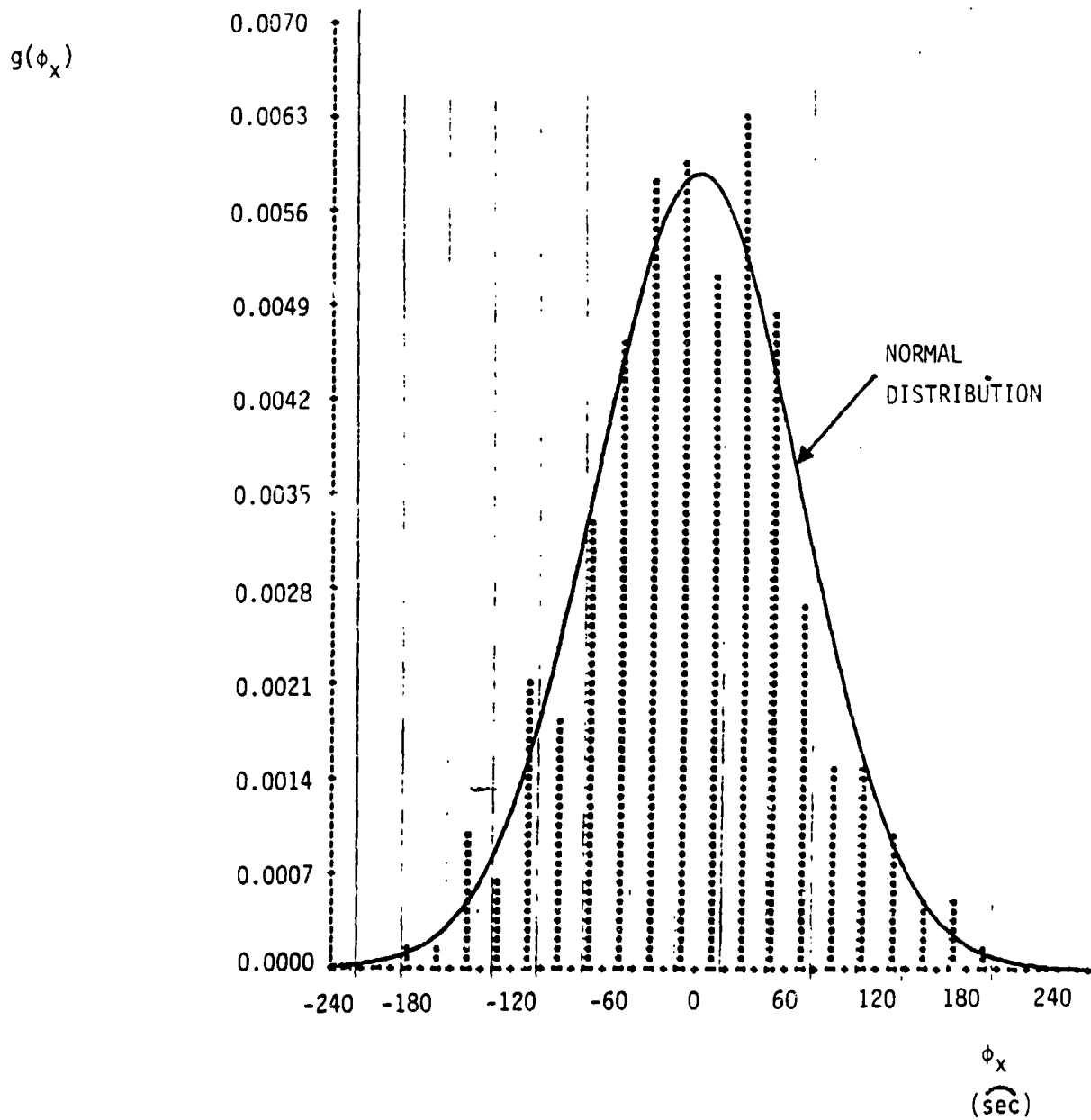


FIGURE C-3 Y-AXIS IMU ALIGNMENT ERROR  
PROBABILITY DENSITY FUNCTION

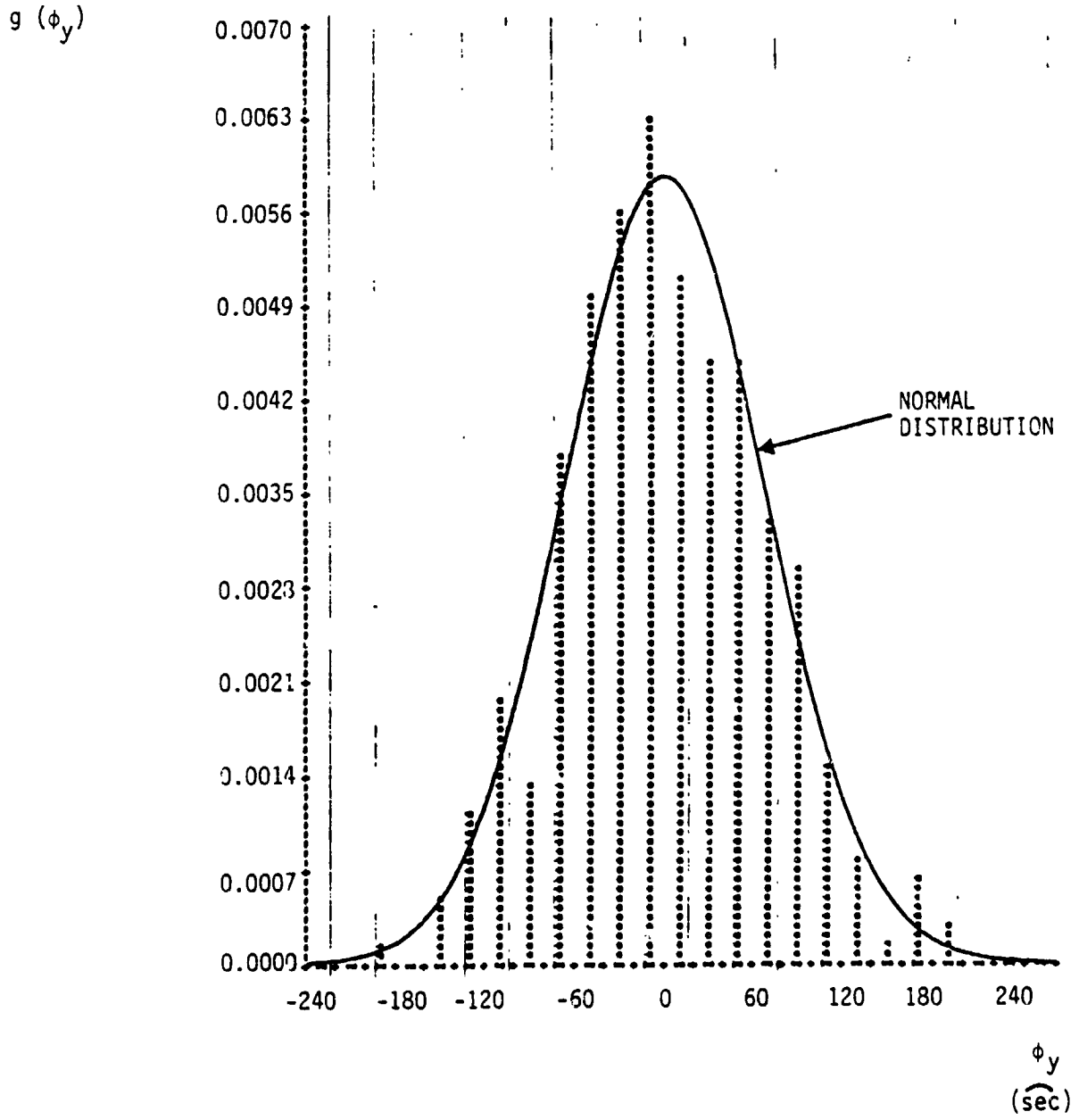
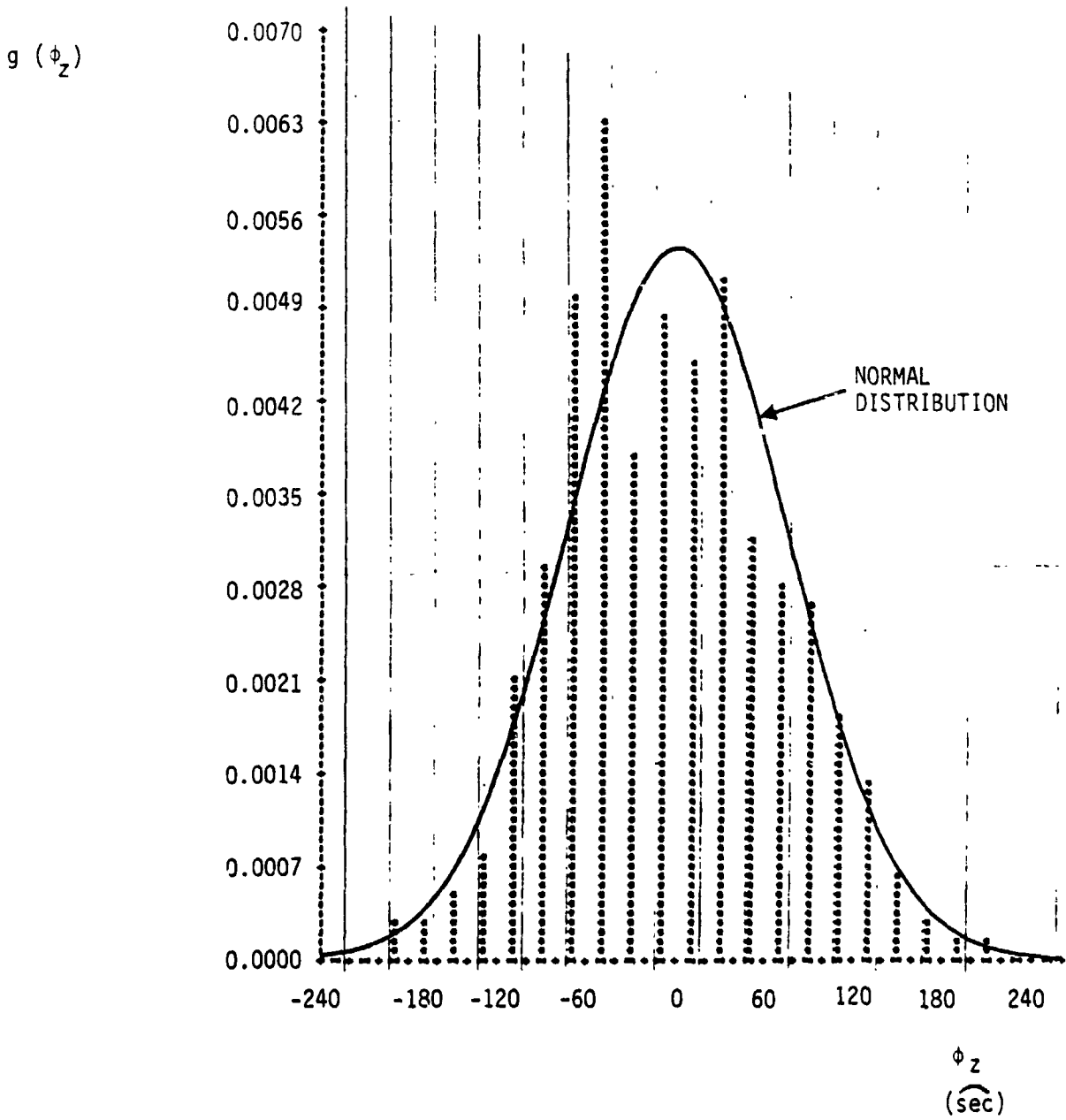


FIGURE C-4 Z-AXIS IMU ALIGNMENT ERROR  
PROBABILITY DENSITY FUNCTION



ORIGINAL PAGE IS  
OF POOR QUALITY

APPENDIX D  
DERIVATION OF THE RMS IMU ALIGNMENT  
ERROR INDICATOR

## D.0 THE RMS IMU ALIGNMENT ERROR

The RMS IMU alignment error indicator is an analytical tool that can be used for estimation of the IMU alignment accuracy. The RMS indicator was first introduced in Reference 2 and it is the purpose of this appendix to present the derivation of this alignment error indicator.

### D.1 DERIVATION OF ALIGNMENT ERROR INDICATOR

Recall that the alignment error is completely defined by the rotation vector  $\Phi$ . It was shown in Reference 2 that with the proper choice of coordinate system, the components of  $\Phi$  can be determined as a function of the alignment star pair angular separation  $\delta$ , the age of the most recently sighted star  $t_s$ , the age of the oldest star sighting  $t_t$ , the star direction measurement errors  $S_{\perp}$ ,  $S_{\parallel}$ ,  $T_{\perp}$ ,  $T_{\parallel}$ , and the IMU drift rates  $d_x$ ,  $d_y$ ,  $d_z$ .

$$\begin{aligned}\phi_x &= \frac{1}{2}(S_{\perp} - T_{\perp} + (t_s + t_t) d_x \sin \frac{1}{2}\delta + (t_s - t_t) d_y \cos \frac{1}{2}\delta) / \sin \frac{1}{2}\delta \\ \phi_y &= \frac{1}{2}(S_{\perp} + T_{\perp} + (t_s - t_t) d_x \sin \frac{1}{2}\delta + (t_s + t_t) d_y \cos \frac{1}{2}\delta) / \cos \frac{1}{2}\delta \quad (D-1) \\ \phi_z &= S_{\parallel} + t_s d_z\end{aligned}$$

The coordinate system used is fixed relative to the alignment star direction vectors  $S$  and  $T$ . These vectors define a plane referred to as the pair plane. The X-axis of this coordinate system lies in the pair plane and bisects the acute angle between  $S$  and  $T$ . The Z-axis is perpendicular to the pair plane (positive toward  $S \times T$ ) and the Y-axis completes the right angle triad.  $S_{\perp}$  and  $S_{\parallel}$  are the star measurement angular error components perpendicular and parallel to the pair plane, respectively, for the most recently sighted star  $S$ . Both  $S_{\perp}$  and  $S_{\parallel}$  are normal to the star direction  $S$ . Similarly,  $T_{\perp}$  and  $T_{\parallel}$  are the star measurement angular error components for the oldest star  $T$ . Finally,  $d_x$ ,  $d_y$ , and  $d_z$  are the components of the IMU drift rate about the coordinate axes  $X$ ,  $Y$ , and  $Z$ , respectively.

In the automatic star acquisition mode, IMU alignments will usually be performed immediately following the acquisition of the second star. Hence, this is the case that is of most interest. If the age of the most recently sighted star is negligible ( $t_s = 0$  and  $t_t = t$ ), then equation D-1 simplifies to:

$$\begin{aligned}\phi_x &= \frac{1}{2}(S_{\perp} - T_{\perp} + t d_x \sin \frac{1}{2}\delta - t d_y \cos \frac{1}{2}\delta) / \sin \frac{1}{2}\delta \\ \phi_y &= \frac{1}{2}(S_{\perp} + T_{\perp} - t d_x \sin \frac{1}{2}\delta + t d_y \cos \frac{1}{2}\delta) / \cos \frac{1}{2}\delta \quad (D-2) \\ \phi_z &= S_{\parallel}\end{aligned}$$

The parameters  $\delta$  and  $t$  are referred to as the spatial and temporal separations of the alignment stars, respectively and are predetermined for a given pair of star measurements. The system errors  $S_{\perp}$ ,  $S_{\parallel}$ ,  $T_{\perp}$ ,  $T_{\parallel}$ ,  $d_x$ ,  $d_y$ , and  $d_z$ , on the other hand, are random variables which cause the alignment error vector components to be random variables also. The star direction measurement errors,  $S_{\perp}$ ,  $S_{\parallel}$ ,  $T_{\perp}$ , and  $T_{\parallel}$ , are all assumed to be normally distributed, independent random variables with zero means. Since these errors are the sum of a large number of random components (Reference 1), the Central Limit Theorem makes this a reasonable assumption. The IMU drift rates,  $d_x$ ,  $d_y$ ,  $d_z$ , are

also assumed to be normally distributed, independent random variables with zero means. Additionally, the measurement errors and the drift rates are assumed to be isotropic in three space. The expectations and the variances of these random variables are summarized by the following equations:

$$\begin{aligned}
 E(S_{\perp}) &= E(S_{\parallel}) = E(T_{\perp}) = E(T_{\parallel}) = 0 \\
 V(S_{\perp}) &= V(S_{\parallel}) = V(T_{\perp}) = V(T_{\parallel}) = \sigma_0^2 \\
 E(d_x) &= E(d_y) = E(d_z) = 0 \\
 V(d_x) &= V(d_y) = V(d_z) = \sigma_d^2
 \end{aligned}
 \tag{D-3}$$

Given the aforementioned assumptions and the properties defined by equations D-2 and D-3, it can be shown that the alignment error components are also independent and normally distributed with expectations and variances defined as follows:

$$\begin{aligned}
 E(\phi_x) &= \mu_x = 0 \\
 E(\phi_y) &= \mu_y = 0 \\
 E(\phi_z) &= \mu_z = 0 \\
 V(\phi_x) &= \sigma_x^2 = \frac{1}{2}(\sigma_0^2 + \frac{1}{2} t^2 \sigma_d^2) / \sin^2 \frac{1}{2} \delta \\
 V(\phi_y) &= \sigma_y^2 = \frac{1}{2}(\sigma_0^2 + \frac{1}{2} t^2 \sigma_d^2) / \cos^2 \frac{1}{2} \delta \\
 V(\phi_z) &= \sigma_z^2 = \sigma_0^2
 \end{aligned}
 \tag{D-5}$$

The joint probability density function (pdf) for the alignment error components, therefore, is defined by:

$$f(\phi_x, \phi_y, \phi_z) = \frac{1}{(2\pi)^{3/2} \sigma_x \sigma_y \sigma_z} e^{-\frac{1}{2} \left[ \frac{\phi_x^2}{\sigma_x^2} + \frac{\phi_y^2}{\sigma_y^2} + \frac{\phi_z^2}{\sigma_z^2} \right]}
 \tag{D-6}$$

Although this function completely defines the properties of the alignment error vector  $\phi$ , it is not very useful for several reasons. First of all, this function describes the alignment error properties in a coordinate system fixed relative to the star directions. The alignment error properties are most useful if they can be related to the IMU platform coordinate system or the Mean-of-1950 Shuttle reference inertial coordinate system. These two systems can assume any orientation relative to the alignment star pair. The directional characteristics of the alignment error vector, however, are of secondary importance. Of primary interest is the magnitude of the alignment error vector which is given by

$$|\phi| = \sqrt{\phi_x^2 + \phi_y^2 + \phi_z^2}
 \tag{D-7}$$

The pdf  $g(|\phi|)$  is the panacea for alignment error estimation because it is independent of the choice of coordinate system. Once the pdf  $g(|\phi|)$  is known, then the expectation and the variance of  $|\phi|$  can be determined.



Unfortunately, there is no closed form solution for  $g(|\Phi|)$ .

The RMS IMU alignment error indicator is a serviceable alternative to this dilemma. Recall that the expectation and the variance of a random variable are related by

$$E(|\Phi|^2) = V(|\Phi|) + E(|\Phi|)^2 \quad (D-8)$$

In the adopted notation, this is equivalent to

$$\omega^2 = \sigma^2 + \mu^2 \quad (D-9)$$

Although  $\mu$  and  $\sigma$  cannot be solved for individually, the sum of  $\mu^2$  and  $\sigma^2$  can be solved for. The expectations of the squares of both sides of equation D-7 is

$$\begin{aligned} E(|\Phi|^2) &= E(\phi_x^2 + \phi_y^2 + \phi_z^2) \\ E(|\Phi|^2) &= E(\phi_x^2) + E(\phi_y^2) + E(\phi_z^2) \\ E(|\Phi|^2) &= V(\phi_x) + E(\phi_x)^2 + V(\phi_y) + E(\phi_y)^2 + V(\phi_z) + E(\phi_z)^2 \end{aligned} \quad (D-10)$$

Since the error components have zero means (equation D-4), equation D-10 simplifies to

$$E(|\Phi|^2) = V(\phi_x) + V(\phi_y) + V(\phi_z) \quad (D-11)$$

which in terms of the adopted notation can be written as

$$\omega^2 = \sigma_x^2 + \sigma_y^2 + \sigma_z^2 \quad (D-12)$$

By combining equations D-5 and D-12, the RMS IMU alignment error,  $\omega$ , can be expressed in terms of the spatial and temporal star pair separations as follows

$$\omega = \sqrt{\sigma_0^2 (1 + 2 \csc^2 \delta) + \sigma_d^2 t^2 \csc^2 \delta} \quad (D-13)$$

## D.2 THE STS-1 CASE

Recall that in Section D.1 it was stated that the pdf of the IMU alignment error magnitude  $g(|\Phi|)$  could not be solved for in closed form. For a single specific case,  $g(|\Phi|)$  can be determined. When IMU alignments are performed during STS-1, the spatial and temporal star pair separations will be optimal.

$$\delta = 90^\circ$$

$$t = 0 \text{ min}$$

In this case, the variances of the alignment error components (equation D-5) are simply

$$\sigma_x^2 = \sigma_0^2$$

$$\sigma_y^2 = \sigma_0^2$$

$$\sigma_z^2 = \sigma_0^2$$

The component errors are normally distributed with equal variances and zero means. The pdf of  $|\Phi|$ , therefore, is defined by Maxwell's distribution.

$$g(|\Phi|) = \sqrt{\frac{2}{\pi}} \frac{|\Phi|^2}{\sigma_0^3} e^{-\frac{1}{2} \left[ \frac{|\Phi|^2}{\sigma_0^2} \right]} \quad (D-14)$$

This function is plotted and superimposed on the simulation derived pdf in Appendix C. The probability density functions for the single axis alignment errors about the X, Y, and Z platform axes are also included in Appendix C. The expectation and the variance of the Maxwell distribution are defined by

$$E(|\Phi|) = 2\sigma_0 \sqrt{2/\pi} \quad (D-15)$$

$$V(|\Phi|) = \sigma_0^2 [3 - 8/\pi] \quad (D-16)$$